ELSEVIER

International Journal of Mass Spectrometry 176 (1998) 1–12

International Journal of Mass Spectrometry

Chemical kinetics of yttrium ionization in H_2–O_2–N_2 flames

QingFeng Chen, John M. Goodings*

Department of Chemistry, York University, 4700 Keele Street, North York, Ontario M3J 1P3, Canada

Received 22 October 1997; accepted 6 February 1998

Abstract

Trace amounts ($\leq 10^{-6}$ mol fraction) of yttrium were introduced into six H_2–O_2–N_2 flames in the temperature range 1820–2400 K at atmospheric pressure. Metallic ions were observed by sampling the flames through a nozzle into a mass spectrometer, and were measured as profiles of ion concentration vs. distance (i.e. time) along the flame axis. The ions observed conform to a series $YO^+ \cdot nH_2O$ (n = 0–3); YO^+ is barely detectable, $Y(OH)_2^+$ with n = 1 is the dominant ion, and the higher hydrates are produced by cooling that occurs during sampling. The major yttrium neutral species are the oxide–hydroxide OYOH (>80%) and the oxide YO (<20%). By the addition of 0.25 mol % of CH_4 and a trace of potassium, it was possible to boost the ionization level appropriately to make electron-ion recombination of $Y(OH)_2^+$ the dominant process; values of the recombination coefficient $(9.7 \pm 1.5)T^{-2.3\pm0.6}$ cm^3 molecule^{-1} s^{-1} were obtained. A radical species such as H in these flames can overshoot its equilibrium concentration by a factor γ of 100 or more in the reaction zone but γ decays downstream towards equilibrium. Neutral OYOH and YO, whose concentrations depend on γ, are linked by the balanced reaction YO + H_2O = OYOH + H having an equilibrium constant K = exp(−49,000/RT). This leads to a bond energy value D^0(OY–OH) = 449 ± 20 kJ mol^{-1}. Analysis of the ion profiles as a function of γ is helpful in ascertaining the ion formation processes. Yttrium ions are produced by the chemi-ionization reaction of OYOH with H; because the ionization energy of YO is low, a small contribution (<1%) might arise from collisional (thermal) ionization of YO. The rate constant for chemi-ionization was found to be $(2.7 \pm 0.8) \times 10^{-12}$ exp(−22452/T) cm^3 molecule^{-1} s^{-1}. This rate constant should be regarded as a lower limit because a fraction of the total yttrium, presumably small, may be present in these flames as solid particles. (Int J Mass Spectrom 176 (1998) 1–12) © 1998 Elsevier Science B.V.

Keywords: Chemi-ionization; Flame ionization; Kinetics; Mass spectrometry; Yttrium

1. Introduction

In 1995, we reported a study concerned with the ionization of the group 3 (or 3B) metals La, Y, and Sc in H_2–O_2–Ar flames [1] followed by a similar study of the lanthanide metals Ce, Pr, and Nd [2]. These metals exist in flames almost exclusively as metallic compounds, mainly the oxide AO and the oxide hydroxide OAOH, where A is the metal atom. Hydrogen flames contain very little natural ionization. When these flames were doped with ~10^{-6} mol fraction of metal, the observation of appreciable ion signals indicated that metallic ions were produced by chemi-ionization or collisional (thermal) ionization reactions. The metallic ion signals could also be enhanced by adding about 0.2 mol % of a hydrocarbon to the flame gas; this technique produces the natural flame ion H_3O^+ (present in super-equilibrium concentrations) that reacted with the compounds to give metallic ions by

* Corresponding author.

PII S1387-3806(98)14013-7

Table 1
Properties of the hydrogen–oxygen–nitrogen flames

Property	Flame number					
	2	25	3	4	5	7
Equivalence ratio ϕ	1.5	1.5	1.5	1.5	1.5	0.75
$H_2/O_2/N_2$	2.74/1/2.95	3.0/1/3.5	3.18/1/4.07	3.09/1/4.74	3.12/1/5.77	1.5/1/3.55
Total unburnt gas flow ($cm^3\ s^{-1}$)	300	250	250	200	150	250
Measured flame temperature (K)	2400	2230	2080	1980	1820	2080
Rise velocity ($m\ s^{-1}$)	19.8	18.6	15.6	11.4	8.4	13.2
Equilibrium burnt gas composition (mol fractions)						
H_2O	0.3460	0.3063	0.2754	0.2553	0.2249	0.2803
H_2	0.1286	0.1527	0.1622	0.1390	0.1259	0.0006640
O_2	0.0001057	0.00000790	0.00000072	0.00000018	0.00000001	0.04443
H	0.006019	0.002650	0.001077	0.0005008	0.0001415	0.00006846
OH	0.003084	0.0007951	0.0002130	0.00008890	0.00001754	0.003242
O	0.00009469	0.00000935	0.00000099	0.00000023	0.00000001	0.0002446
N_2	0.5157	0.5375	0.5610	0.6052	0.6490	0.6668

chemical ionization (CI). The main thrust of these previous studies, which were largely qualitative, was to ascertain the ionization mechanism(s) and to explore the resulting metallic ion chemistry at high temperature in flames.

Our main objective in the present study was to measure quantitative values of rate constants for ion production and loss of any typical one of these metals. Yttrium was chosen because, like La and Sc, it has a relatively simple ion spectrum that can be represented by an oxide ion series $YO^+ \cdot nH_2O$ (n = 0–4); in the case of Y, signals for n = 0 and 4 are very small but the others are readily measureable. Ions were observed by sampling a cylindrical flame along its axis into a mass spectrometer; kinetic data were derived from profiles of ion concentration vs. axial distance (i.e. time). The ionization level was boosted by the addition of a hydrocarbon and an alkali metal was also added to enhance electron-ion recombination of the principal $YO^+ \cdot H_2O$ ion, equivalent to $Y(OH)_2^+$; the recombination coefficient was measured in different flames to investigate its temperature dependence. With regard to ion production, the known concentration dependence of the free radicals H, OH, and O in flames was exploited to show that the chemi-ionization of yttrium is consistent with the reaction of OYOH with H; the temperature dependence of the rate coefficient was measured. The contribution from collisional (thermal) ionization of YO is small if its rate coefficient is in line with the general expression found previously for the alkali metals [3] when the ionization energy $IE^0(YO)$ is substituted. Thermodynamic data are not available for OYOH but the analysis of the results provided a means of estimating the amounts of [OYOH] and [YO] in flames, consistent with a value obtained for the bond energy $D^0(OY–OH)$. The methods employed in this study should be applicable to others of the group 3 (or 3B) and lanthanide series.

2. Experimental

Six premixed, laminar, $H_2–O_2–N_2$ flames at atmospheric pressure were employed for this work, five of them of fuel-rich composition (FR, equivalence ratio ϕ = 1.5) spanning a temperature range 1820–2400 K, and the sixth fuel lean (FL, i.e. oxygen rich, ϕ = 0.75) having the same temperature as the middle one of the FR set. Their properties including the calculated compositions of the equilibrium burnt gas based on the JANAF Tables [4] are given in Table 1. These flames have been used extensively by Hayhurst and co-workers who have measured their temperatures, rise velocities, and free-radical compositions [5]. The concentrations of free radicals overshoot their equilibrium values in the flame reaction zone and then decay downstream towards equilibrium in the burnt

gas. For FR flames where H_2O and H_2 are major product species, Sugden's disequilibrium parameters [6], $\gamma_H = \gamma_{OH} \equiv \gamma$ and $\gamma_0 = \gamma^2$, are defined as the ratio of the local concentration of a radical at a given position in the flame to its final equilibrium value given in Table 1; γ can achieve large values (>100) close to the reaction zone of the cooler flames before decaying downstream in the burnt gas towards unity. Plots of γ versus axial distance z are available for the five FR flames listed in Table 1 [5]; thus, the radical concentrations are known at all points in the flames. These pseudo-one-dimensional (flat) flames were stabilized on a water-cooled brass burner previously described [7], consisting basically of a circular bundle of 151 stainless-steel hypodermic needle tubes. The FR flames were cylindrical in shape with a diameter of about 12 mm; the FL flame was more conical, reaching an apex some 30–35 mm downstream of the burner.

Yttrium was introduced into the flames by spraying an aqueous solution of $YCl_3 \cdot 6H_2O$ (Aldrich, 99.9%) as an aerosol derived from an atomizer described previously [8] into the nitrogen supply of the premixed flame gas. Spraying a 0.1 M solution introduced 9.5×10^{-7} mol fraction of total yttrium into the unburnt flame gas. A small amount of a white solid, presumably yttria Y_2O_3 with a melting point of 2683 K [9], condensed onto the cooled sampling plate placed in front of the flame. At the 0.1 M concentration level, the flames were colored a deep pinkish red. When viewed from the side, the individual reaction-zone cones associated with each hypodermic needle tube were of a paler color, and extended 2–3 mm into the burnt gas. This extension is further than that normally noted for other colored flames doped, for example, with sodium or barium [1]. There is some evidence that yttrium forms solid particles of involatile oxide in flames [10], although the tendency should be lessened in the reducing atmosphere of the FR flames employed here. Whether the extended reaction-zone cones might be associated with the formation of solid particles or even liquid droplets is not clear. Thus, we do not have any firm evidence for particle formation in these flames doped with yttrium.

The six flames described in Table 1 exhibit only a low level of natural ionization. It was sometimes advantageous to add 0.25 mol % of CH_4 to the premixed flame gas to produce a high initial concentration of H_3O^+ ions by chemi-ionization near the flame reaction zone; these ions subsequently decay downstream by electron-ion recombination. With the simultaneous addition of yttrium, H_3O^+ can produce yttrium ions by chemical ionization (CI) processes. The addition of CH_4 was small enough, however, so that the flame composition and temperature remained essentially unchanged. In other cases, it was occasionally desirable to add a small amount of KNO_3 to the yttrium solution sprayed by the atomizer to produce K^+ and free electrons e^- in the flame by collisional (thermal) ionization. By this means, the electron-ion recombination rate of the yttrium ions could be increased; there was no apparent reaction of K^+ with the yttrium ions. That is, yttrium ionization could be enhanced early in the flame by methane and/or depleted later in the flame by potassium.

The burner is mounted horizontally on a motorized carriage with calibrated drive coupled to the *X* axis of an *XY* recorder. The flame axis *z* is accurately aligned with the sampling nozzle of the mass spectrometer. The apparatus has been described in detail previously [7] so only a brief description will be given here. Flame gas containing ions is sampled through an orifice of 0.17 mm diameter. The circular orifice is contained in a tiny electron microscope lens of Pt/Ir alloy swaged into the tip of a conical nozzle protruding from a water-cooled sampling plate of stainless steel. The ions enter a first vacuum chamber maintained at 0.04 Pa (3×10^{-4} torr), and are focused into a beam by an electrostatic lens. The beam then passes through a 3 mm orifice in the tip of a nose cone into a second vacuum chamber pumped to a pressure below 0.003 Pa (2×10^{-5} torr). The ions traverse a second ion lens into a quadrupole mass filter in which they have an axial ion energy of 15 eV. They are detected by a Faraday collector connected to a vibrating-reed electrometer having a grid-leak resistance of 10^{10} Ω; the ion signal is applied to the *Y* axis of the *XY* recorder. Thus, ion signal magnitudes quoted in the figures below as a voltage (in mV) refer to the

collected ion current passing through 10^{10} Ω. By driving the flame towards the sampling nozzle, profiles may be obtained of an individual ion signal vs. distance along the flame axis z. The zero on the X-axis distance scale ($z = 0$) is defined experimentally where the pressure abruptly rises when the sampling nozzle pokes through the flame reaction zone into the cooler unburnt gas upstream. The pressure is measured with an ionization gauge mounted on the second vacuum chamber.

As an alternative to individual ions, total positive ion (TPI) profiles can be measured by switching off the dc voltages to the quadrupole rods. Still, with the dc voltages switched off and the spectrometer's mass dial set to a given mass number, all of the ions above that mass number are collected; e.g. TPI_{90} designates total positive ions above 90 u, whereas TPI_{12} includes all the ions (because no flame ions exist below 12 u). This technique is useful in separating total yttrium ions from ions of low mass number such as H_3O^+, K^+, and Na^+, if present. However, the sensitivity of the mass spectrometer is different for individual ions and TPI because the former are measured at fairly high resolution, whereas total ion collection amounts to zero resolution. The former sensitivity is approximately one half of the latter. It should be pointed out that negative ions were never detected in the FR flames. Because a flame is a quasi-neutral plasma, [TPI] is equal to $[e^-]$, the concentration of free electrons. Calibration procedures for the atomizer delivery into the flame gas and for the mass spectrometer sensitivity have been given previously [11,12]. When the gas is sampled through the nozzle, it cools in two regions: in the thermal boundary layer surrounding the orifice and in the near-adiabatic expansion downstream of the nozzle throat. This can cause a shift of fast equilibrium reactions in the exothermic direction during sampling. In particular, ion hydrates can be enhanced with respect to the parent ion. These sampling problems have been discussed in considerable detail [13–15]. They are obviated in the present study by measuring TPI_{90} such that hydrate contributions are included in the $Y(OH)_2^+$ parent ion signal.

3. Results and discussion

3.1. Neutral yttrium species in flames

As a group 3 (or 3B) metal in the +3 oxidation state, yttrium might be expected to form compounds in flames such as oxides YO and perhaps YO_2, hydroxides $Y(OH)_n$ with $n = 1–3$ and the oxide–hydroxide OYOH in addition to atomic Y. These metals form very strong metal-oxide bonds; for yttrium D_0^0 $(Y–O) = 715 \pm 11$ kJ mol^{-1} (7.41 ± 0.11 eV) [16] such that the monoxide is a stable radical species. Thermodynamic data are not available for most of the other species. However, we have argued previously that [Y] is negligible in these flames [1]; from crude estimates of the relevant bond strengths, the concentrations of the hydroxides are also negligible. Apart from YO, the oxide–hydroxide should be a major species formed by the balanced reaction

$$YO + H_2O \rightleftarrows OYOH + H \quad (1)$$

as was shown to be the case for the group 13 (or 3A) metal aluminum in flames [17] by using available thermodynamic data [4]. Also for aluminum, AlOH is a fairly major species, but not AlO whose bond strength is much less than that of YO; back donation of electron density from the O atom to form the very strong Y–O bond argues against the formation of appreciable YOH. The alternative process for the formation of OYOH involving the three-body association of OH with YO will not be competitive with reaction (1). This conclusion is based on Sugden's general criterion [18] that reaction (1) will be dominant provided the dissociation energy, in this case D^0(OY–OH), exceeds a certain critical value originally estimated to be ~335 kJ mol^{-1}. An estimate of D^0(OY–OH) is provided by the second (much weaker) bond energy of YO_2, namely, D_0^0(OY–O) = 399 ± 21 kJ mol^{-1} (4.14 ± 0.22 eV) [19] such that Sugden's criterion is fulfilled. The existence of YO_2 itself in FR flames is not anticipated, being such a highly oxidized species. Even if it were to form, it would be an odd-electron species of high reactivity that would not be expected to survive in flames; this

is different from YO, another odd-electron species of high chemical stability. In summary, it is concluded that neutral yttrium is present in these flames almost entirely as YO and OYOH. The problem is to ascertain the relative amounts.

A first crude estimate of the neutrals at equilibrium can be made by setting the equilibrium constant $K_1 = \exp(-\Delta G_1^0/RT)$ for reaction (1) with $\Delta G_1^0 \approx \Delta H_1^0 = D^0(\text{H–OH}) - D^0(\text{OY–OH})$ and assuming $D^0(\text{OY–OH}) \approx D^0(\text{OY–O})$; $D^0(\text{H–OH}) = 498 \pm 4$ kJ mol^{-1} (5.16 ± 0.04 eV) [9]. By using the equilibrium concentrations from Table 1, this estimate gives [OYOH]/[YO] = $K_1[H_2O]/[H]$ ranging from 28.7%/71.3% in flame 2 to 69.6%/30.4% in flame 5; the ratio is 93.0%/7.0% in FL flame 7, higher because [H] is low. However, the ratio will steadily increase downstream of the reaction zone in a flame because [H] decreases as the disequilibrium parameter γ falls towards unity; i.e. [H] decreases to $[H]_{eq}$, the equilibrium concentration. At any point in a flame, the actual concentration of OYOH or YO can be expressed in terms of the total yttrium concentration $[Y_{tot}]$ = [OYOH] + [YO] as a function of γ. In the FR case where $[H] = \gamma[H]_{eq}$, these concentrations are given by Eqs. (1a) and (1b) related to reaction (1)

$$[\text{OYOH}] = \frac{[Y_{tot}]K_1[H_2O/[H]_{eq}}{\gamma + K_1[H_2O]/[H]_{eq}} \quad (1a)$$

$$[\text{YO}] = \frac{[Y_{tot}]\,\gamma}{\gamma + K_1[H_2O]/[H]_{eq}} \quad (1b)$$

such that $[\text{OYOH}]/[\text{YO}] = K_1[H_2O]/\gamma[H]_{eq}$. The γ dependence of OYOH and YO leads to a better value of K_1 than the crude estimate given above, based on curve fitting of the ion chemistry discussed below.

3.2. Recombination of $Y(OH)_2^+$ with electrons

These hydrogen flames contain a small amount of H_3O^+ natural ionization formed by the chemi-ionization reaction [20]

$$H + H + OH \rightleftarrows H_3O^+ + e^- \quad (2)$$

With H_3O^+, OYOH can undergo a chemical ionization (CI) reaction by proton transfer

$$H_3O^+ + \text{OYOH} \rightleftarrows Y(OH)_2^+ + H_2O \quad (3)$$

and YO, which has a low ionization energy $IE_0^0(\text{YO}) = 564 \pm 14$ kJ mol^{-1} (5.85 ± 0.15 eV) [21], can be chemically ionized by electron transfer

$$H_3O^+ + \text{YO} \rightleftarrows \text{YO}^+ + H_2O + H \quad (4)$$

followed by hydration

$$\text{YO}^+ + H_2O + M \rightleftarrows M + \text{YO}^+ \cdot H_2O \text{ or } Y(OH)_2^+ \quad (5)$$

where M is a third body. Reaction (4) is well known in flames for the chemical ionization of metallic atoms having relatively low ionization energies such as the alkali metals [22]. Reaction (5) is rapidly equilibrated in flames because of the high water content in the products. The sum of reactions (4) and (5) amounts to the overall CI reaction

$$H_3O^+ + \text{YO} \rightleftarrows Y(OH)_2^+ + H \quad (6)$$

Note that reactions (3) and (6) have the same product ion $Y(OH)_2^+$, which is always the principal yttrium ion observed with the mass spectrometer apart from small signals due to ion hydrates formed by cooling during sampling. Reproductions of actual ion profiles traced on the XY recorder are shown in Fig. 1(a) for the FR flame 3 and in Fig. 1(b) for the FL flame 7 at the same temperature of 2080 K with the atomizer spraying a 0.075 M solution of $YCl_3 \cdot 6H_2O$.

In addition to CI, further reactions for the production of $Y(OH)_2^+$ ions by chemi-ionization and collisional (thermal) ionization are considered in the next section. It is first desirable to consider their loss by electron-ion recombination; the recombination coefficient is required to evaluate the rate constant(s) for production. The objectives here were to form a relatively high concentration of $Y(OH)_2^+$ rapidly near the flame reaction zone and then to assure that the recombination reaction

$$Y(OH)_2^+ + e^- \rightarrow \text{neutral products} \quad (7)$$

was dominant downstream in the burnt gas. These were achieved, first by adding 0.25 mol % of CH_4 to produce a superequilibrium level of H_3O^+ that chem-

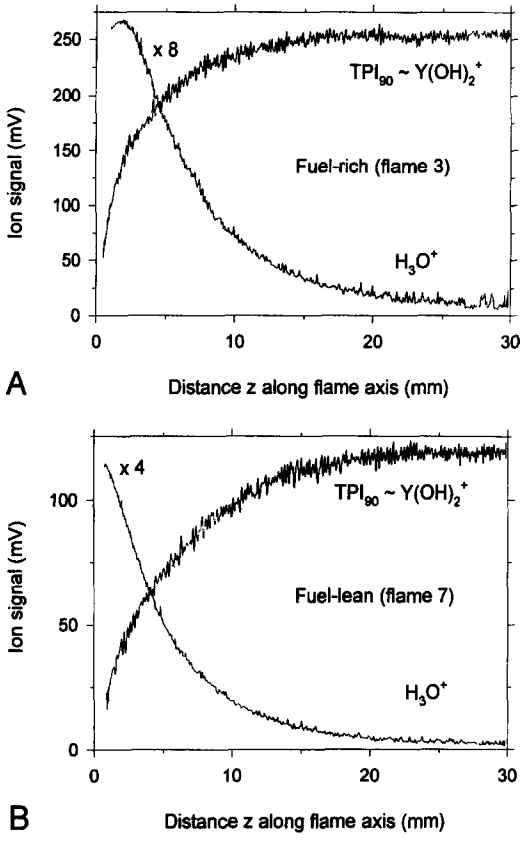

Fig. 1. Ion profiles of $Y(OH)_2^+$ and H_3O^+ measured along the flame axis with the atomizer spraying a 0.075 M solution of $YCl_3 \cdot 6H_2O$ (A) in the fuel-rich flame 3, and (B) in the fuel-lean flame 7, both at the same temperature of 2080 K.

ically ionizes yttrium to form a high initial $Y(OH)_2^+$ signal by reactions (3) and (6). Then, a small amount of potassium as KNO_3 was added to the atomizer solution to raise the concentration of free electrons in the flame, thereby enhancing the rate of recombination of $Y(OH)_2^+$ by reaction (7). Potassium atoms are chemically ionized initially by H_3O^+ to some extent [22]

$$H_3O^+ + K \rightarrow K^+ + H_2O + H \quad (8)$$

but progressively ionize further downstream by collisional (thermal) ionization [3]

$$K + M \rightleftarrows K^+ + e^- + M \quad (9)$$

There is no evidence that potassium interacts with yttrium by any process other than its effect on

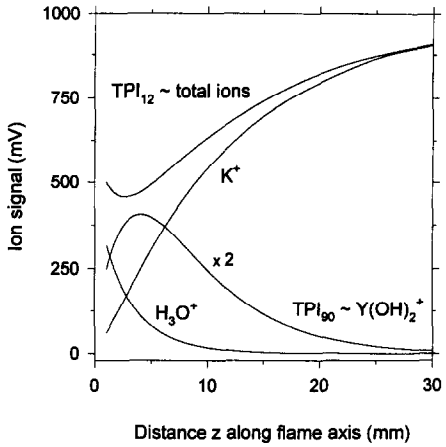

Fig. 2. Ion profiles along the axis of flame 25 with 0.25 mol % of added CH_4 and with the atomizer spraying a solution of 0.0875 M $YCl_3 \cdot 6H_2O$ and 0.000625 M KNO_3 such that electron-ion recombination of $Y(OH)_2^+$ is the dominant process downstream.

recombination through $[e^-]$. It was necessary to adjust the concentrations of both $YCl_3 \cdot 6H_2O$ and KNO_3 in the atomizer solution rather carefully so that (i) H_3O^+ disappears quite rapidly downstream to maximize the region in which $Y(OH)_2^+$ recombination is dominant, and (ii) $[Y(OH)_2^+]$ falls to a value near zero at $z = 30$ mm downstream, indicating that yttrium ion production by chemi-ionization and/or collisional (thermal) ionization is negligible.

Figure 2 presents profiles for flame 25 with added CH_4 and with the atomizer spraying a mixed aqueous solution of 0.0875 M $YCl_3 \cdot 6H_2O$ and 0.000625 M KNO_3. At these concentrations, the profiles fulfill the conditions outlined in (i) and (ii) above. The TPI_{90} signal includes $Y(OH)_2^+$ and any hydrates formed during sampling. Because negative ions are negligible in these flames, the TPI_{12} profile that measures the sum of all positive ions gives $[e^-]$ because a flame is a quasi-neutral plasma. From reaction (7), $-d[Y(OH)_2^+]/dt = k_7[Y(OH)_2^+][e^-]$ − (ion production term) with $v = dz/dt = 18.6$ m s^{-1} from Table 1. Figure 3 shows a plot of $-d[Y(OH)_2^+]/dz$ vs. $[Y(OH)_2^+][e^-]$, which gives a good straight line in the range $z = 10$ to 30 mm having a slope k_7/v; the value of the recombination coefficient $k_7 = 1.8 \times 10^{-7}$ cm^3 molecule^{-1} s^{-1}. The fact that the straight line

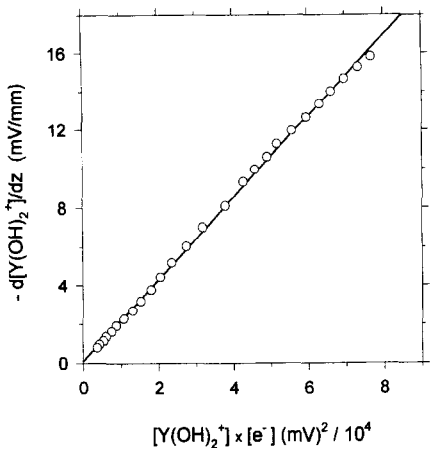

Fig. 3. Plot of $-d[Y(OH)_2^+]/dz$ vs. $[Y(OH)_2^+] \times [e^-]$ in the range z = 10–30 mm by using the profiles from Fig. 2 for flame 25 with 0.25 mol % of added CH_4 and with the atomizer spraying a solution of 0.0875 M $YCl_3 \cdot 6H_2O$ and 0.000625 M KNO_3.

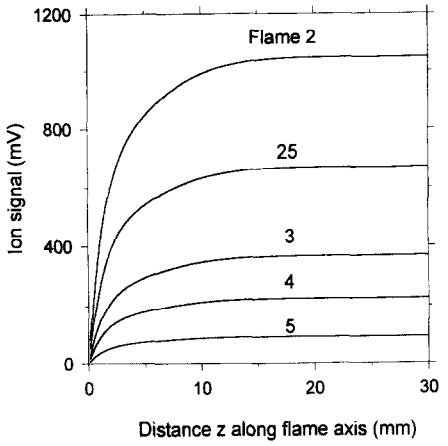

Fig. 5. Ion profiles with the signal measured as TPI_{90} along the axis of the five fuel-rich flames with the atomizer spraying a 0.1 M solution of $YCl_3 \cdot 6H_2O$ where equilibrium of the yttrium ions is attained downstream.

passes almost through the origin shows that ion production is very small under the conditions chosen.

The same procedures were carried out for all five FR flames listed in Table 1 spanning a temperature range from 1820 to 2400 K. The results of many determinations of the recombination coefficient are given in Fig. 4 as a plot of log k_7 versus log T. The least-squares fit of a straight line through the data points gives $k_7 = (9.7 \pm 1.5)T^{-2.3\pm0.6}$ cm^3 molecule^{-1} s^{-1} with a negative temperature dependence. A discussion of the temperature dependence of electron-ion recombination coefficients in the context of flames has been given by Butler and Hayhurst [23]. Simple theory indicates a $T^{-1.5}$ dependence with which our value is in approximate agreement.

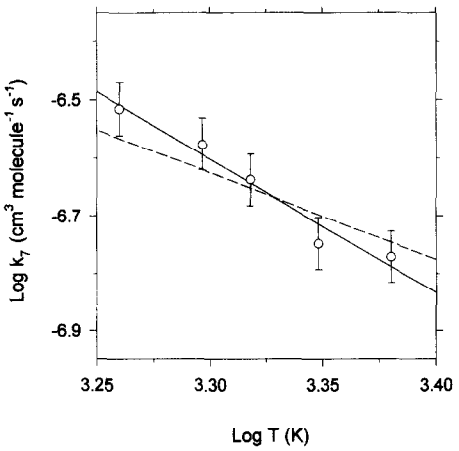

Fig. 4. Logarithmic plot of the recombination coefficient k_7 vs. temperature T in the range 1820–2400 K. The best-fit solid line exhibits a $T^{-2.3}$ dependence, for comparison with the dashed line giving the $T^{-1.5}$ dependence expected from simple theory.

3.3. Production of $Y(OH)_2^+$ ions

Profiles for total yttrium ionization measured as TPI_{90} are presented in Fig. 5 for the five FR flames with the atomizer spraying a 0.1 M solution of $YCl_3 \cdot 6H_2O$. At this relatively high concentration, each profile rises near the reaction zone and then reaches a constant plateau value downstream, indicative of equilibrium for ion production and ion loss. Several processes for yttrium ion production have been considered [1]. The chemi-ionization reaction of atomic species studied by Dyke and his co-workers for lanthanide metals [24]

$$Y + O \rightleftarrows YO^+ + e^- \quad (10)$$

followed by reaction with water

$$YO^+ + H_2O + M \rightleftarrows Y(OH)_2^+ + M \quad (5)$$

is not feasible in flames because, as mentioned in Sec. 3.1 above, [Y] is extremely small. Also, $[YO^+]$ is

very small and could only be observed at the limit of detection of the mass spectrometer. The relatively low ionization energy for YO of 5.85 eV [21] makes it a logical candidate for collisional (thermal) ionization

$$YO + M \rightleftarrows YO^+ + e^- + M \quad (11)$$

followed by the hydration reaction (5) to yield $Y(OH)_2^+$. The direct formation of $Y(OH)_2^+$ by chemi-ionization of OYOH without invoking the presence of YO^+

$$OYOH + H \rightleftarrows Y(OH)_2^+ + e^- \quad (12)$$

is a likely mechanism because [OYOH] is large. As discussed previously [1], reactions (11) and (12) are linked by a cyclic reaction scheme

$$YO + H_2O \underset{(1)}{=} OYOH + H \quad (13)$$

$$(11) \uparrow \downarrow M \qquad \uparrow \downarrow (12)$$

$$YO^+ + e^- + H_2O \underset{(5)}{\overset{(M)}{=}} Y(OH)_2^+ + e^-$$

such that reaction (12) = (−1) + (11) + (5). Reactions (1) and (5) have high rates in both directions and are assumed to be rapidly balanced (designated by = sign) in flames.

One further production reaction should probably be considered involving the chemi-ionization of YO

$$YO + H \rightleftarrows YOH^+ + e^- \quad (14)$$

followed rapidly by H atom abstraction to form YO^+

$$YOH^+ + H, OH \rightleftarrows YO^+ + H_2, H_2O \quad (15)$$

with hydration by reaction (5) to give $Y(OH)_2^+$. Conceivably, YOH^+ could react directly with water to produce $Y(OH)_2^+$

$$YOH^+ + H_2O \rightleftarrows Y(OH)_2^+ + H \quad (16)$$

In general, reaction (14) is unlikely because it involves attack by H at the O atom whose electron density has been reduced by back donation to form the very strong Y–O bond; YOH^+ was never observed with the mass spectrometer. Also, it does not lead to the correct magnitudes of the yttrium ion signals. In our previous study [1], it was well established that, for a pair of flames at the same temperature, the FR ion signal always exceeded the FL signal by a factor of 2–4. Figs. 1(a) and 1(b) are a case in point where the measured FR/FL ion ratio is 2.1 at z = 30 mm downstream in flames 3 and 7. However, calculated ratios of $k_{14}[YO][H] = k_7[TPI_{90}]^2$ predict an FR/FL ion ratio of 6.8 that is too large to be credible. In contrast, calculated ratios of $k_{12}[OYOH][H] = k_7[TPI_{90}]^2$ predict a ratio of 2.5, in fairly good agreement with the measurements. These calculations involve Eqs. (1a) and (1b) for [OYOH] and [YO] with $\gamma = 1.5$ downstream in both flames and $K_1 = 0.0588$ at 2080 K, the value taken from the final expression given in the conclusions. It is also important to recognize that, in FL flames where H_2O and O_2 but not H_2 are major species in the products, Sugden's disequilibrium parameters are different. In this case, $\gamma_{OH} \equiv \gamma$ but $\gamma_H = \gamma^3$ and $\gamma_0 = \gamma^2$ [25]; i.e. $[H] = \gamma^3[H]_{eq}$. From these considerations, it is concluded that reaction (14) is not operative to any appreciable extent.

The γ dependence of the $Y(OH)_2^+$ signal in these FR flames is a useful tool for determining the mechanism of ion production. If reaction (12) is responsible for the profiles in Fig. 5, $d[Y(OH)_2^+]/dt = k_{12}[OYOH][H]_{eq}\gamma - k_{-12}[Y(OH)_2^+]^2$ because $[Y(OH)_2^+] = [e^-]$. With $v = dz/dt$, a plot of $v\{d[Y(OH)_2^+]/dz\} + k_{-12}[Y(OH)_2^+]^2$ versus γ should give a straight line through the origin of slope $k_{12}[OYOH][H]_{eq}$; this requires that γ is small compared with $K_1[H_2O]/[H]_{eq}$ in the denominator of Eq. (1a) that can be shown by calculation to be the case. Note that $k_{-12} = k_7$ for recombination. Fig. 6(a) presents such a plot for the profile of flame 3 from Fig. 5 in the range z = 0.2 to 30 mm; the values of γ were taken from Butler and Hayhurst [5]. It is evident that the conditions imposed by reaction (12) are fulfilled. By way of contrast, Fig. 6(b) shows a plot versus γ^2 that should yield a straight line if O atoms were involved (with $\gamma_0 = \gamma^2$) in a chemi-ionization process such as reaction (10); clearly, a straight line is not obtained.

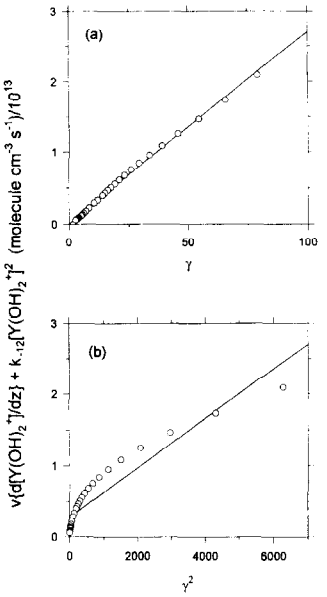

Fig. 6. Plot of the net rate of yttrium ion production in flame 3 vs. functions of the disequilibrium parameter such as (a) γ, and (b) γ^2, to confirm the mechanism of the ion production reaction; the atomizer is spraying a 0.1 M solution of $YCl_3 \cdot 6H_2O$.

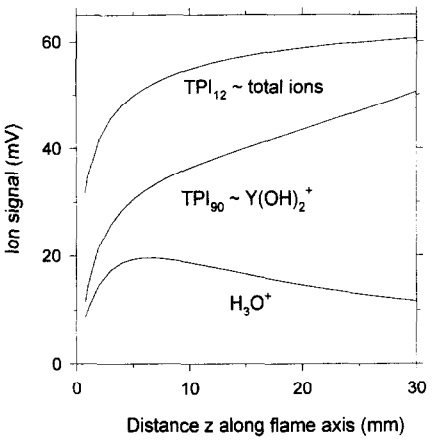

Fig. 7. Profiles in flame 3 of the total positive ions TPI_{12}, the total yttrium ions TPI_{90} and H_3O^+ with the atomizer spraying a 0.02 M solution of $YCl_3 \cdot 6H_2O$ of relatively low concentration so that yttrium ion production dominates over ion loss.

It is evident from Eq. (1b) that reaction (11) for collisional (thermal) ionization of YO exhibits the same γ dependence as that of the chemi-ionization reaction (12). An estimate of k_{11} can be obtained from the general expression worked up by Hayhurst and his co-workers [3] for rate coefficients for thermal ionization of the alkali metals; namely, $k = (9.9 \pm 2.7) \times 10^{-9}\ T^{1/2} \exp(-IE/RT)$ cm^3 molecule^{-1} s^{-1}, where IE is the ionization energy. For example, in flame 3 at 2080 K, $k_{11} = 3.0 \times 10^{-21}$ cm^3 molecule^{-1} s^{-1} with $IE_0^0(YO) = 564 \pm 14$ kJ mol^{-1} (5.85 ± 0.15 eV) [21]. Also, $k_{12} = 6.2 \times 10^{-17}$ cm^3 molecule^{-1} s^{-1} taken from the final expression for k_{12} given in the conclusions. These values indicate that the rate of reaction (11) for thermal ionization is less than 1/3% of the rate of reaction (12). In summary, Fig. 6 is a powerful indicator that yttrium ionization is dominated by the chemi-ionization reaction (12) of OYOH with H.

Values of k_{12} were obtained by two methods, first by spraying the relatively low concentration of 0.02 M $YCl_3 \cdot 6H_2O$ solution in the atomizer to maximize ion production over ion loss. This is in contrast to the second method by using 0.1 M solution to produce the flat equilibrated profiles downstream in Fig. 5. For the 0.02 M solution in flame 3, profiles are given in Fig. 7 for all the total positive ions TPI_{12}, the total yttrium ions TPI_{90} and H_3O^+. Note that at this low concentration, H_3O^+ is present throughout the burnt gas so that yttrium ions may be produced by chemical ionization (CI) via reactions (3) and (4) as well as by chemi-ionization via reaction (12). Also, H_3O^+ ions are produced by the chemi-ionization reaction (2) that has a γ^3 dependence. Curve fitting by using a modified Hoerl regression model ($y = ab^{1/x}x^c$) was applied to the TPI_{12} profile in the range $z = 2$–16 mm where accurate values of γ are available from which the slope of the profile can be obtained at any position z in the flame. The value of k_{12} was found from the total yttrium ion production rate expression $y = v\{d[TPI_{12}]/dz\} + k_{-12}[TPI_{12}]^2 - k_2[H]_{eq}^2[OH]_{eq}\gamma^3 = k_{12}[OYOH][H] = k_{12}\{[Y_{tot}]K_1[H_2O]/(\gamma + K_1[H_2O]/[H]_{eq})\}\gamma$ from Eq. (1a). The expression has the functional form $y = p\gamma/(\gamma + q)$; with $x = \gamma - 1$ ($\gamma \geq 1$ so $x \geq 0$), a Taylor series expansion of the right-hand side cut off after the x^2 term yields a quadratic function $y = a + bx + cx^2$. By using the TPI_{12} profile given in Fig. 7 for flame 3, a plot of the experimental left-hand side of the kinetic rate expres-

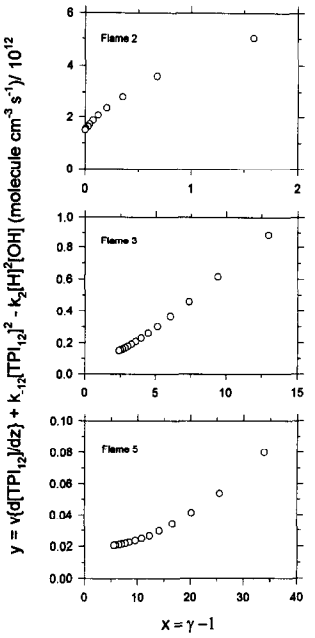

Fig. 8. Plot of the total rate of yttrium ion production vs. the disequilibrium parameter function ($\gamma - 1$) using the TPI_{12} profile of Fig. 7 for flame 3; similar plots are also shown for the hottest flame 2 and the coolest flame 5. The rate constant for chemi-ionization is obtained by fitting a quadratic function to the curves.

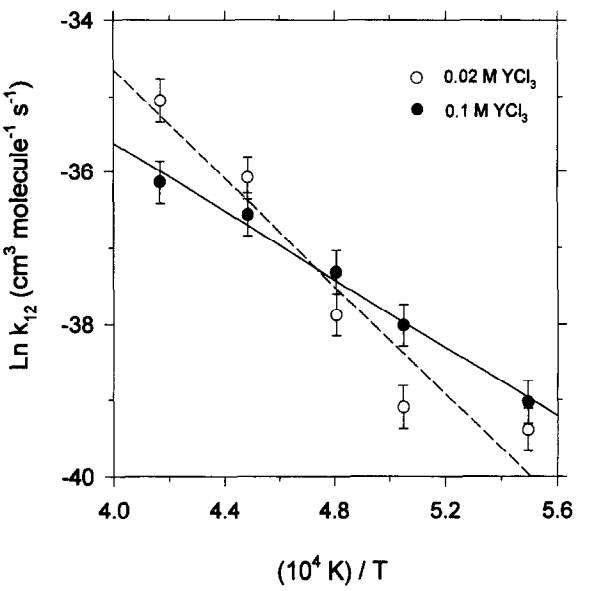

Fig. 9. Semi-logarithmic plots of ln k_{12} for chemi-ionization of OYOH with H vs. inverse temperature obtained by two methods: curve fitting to profiles at low concentration (open circles, broken line), and equilibrium measurements at high concentration (filled circles, solid line).

sion y versus x is shown in Fig. 8; similar plots are also given for the hottest flame 2 and coolest flame 5. The plots show a continuous trend: convex upwards for flame 2, almost linear for flame 3, and convex downwards for flame 5. Each of these plots for the five FR flames gives a very good fit to a quadratic function. Each curve fit yields a, b, and c from which k_{12} and K_1 can be determined. Seemingly good values of k_{12} are obtained that are insensitive to small changes in a, b, and c. However, the values of K_1 are rather erratic, scattered in the range 0.03–0.19. Possibly, the analysis by curve fitting places demands on the data beyond their capabilities.

To clarify K_1, different values of K_1 were introduced into the right-hand side of the kinetic expression, i.e., $y = k_{12}[\mathrm{OYOH}][\mathrm{H}] = k_{12}\{[\mathrm{Y_{tot}}]K_1[\mathrm{H_2O}]/(\gamma + K_1[\mathrm{H_2O}]/[\mathrm{H}]_{eq})\}\gamma$, to obtain the best match of the k_{12} values with those generated above. This occurred for $K_1 = \exp(-49{,}000/RT)$; i.e. $\Delta G_1^0 = 49 \pm 10$ kJ mol^{-1}. It corresponds to equilibrium values of the neutral composition for [OYOH]/[YO] ranging from 83.1%/16.9% in flame 2 to 96.0%/4.0% in flame 5. These data indicate that the OY–OH bond is some 50 kJ mol^{-1} stronger than the OY–O bond energy used above for our first crude estimate, and we conclude that D^0(OY–OH) = 449 ± 20 kJ mol^{-1} (107 ± 5 kcal mol^{-1} = 4.65 ± 0.21 eV).

With $K_1 = \exp(-49{,}000/RT)$, the values of k_{12} obtained by curve fitting change very slightly, and are shown in Fig. 9 as a plot of ln k_{12} versus $1/T$ (open circles, broken line). As an example, the data for flame 3 in Figs. 7 and 8 give a value $k_{12} = 3.5 \times 10^{-17}$ cm^3 molecule^{-1} s^{-1}. At this low concentration of 0.02 M, the recombination correction $k_{-12}[\mathrm{TPI_{12}}]^2$ was small. Likewise, the correction $k_2[\mathrm{H}]^2[\mathrm{OH}]$ for H_3O^+ production was small also. Finally, it should be recognized that CI by H_3O^+ does not alter the kinetic expression for the production of yttrium ions in the range z = 2–16 mm. This is true because H_3O^+ production has been taken into account, and subsequent loss of H_3O^+ to form $Y(OH)_2^+$ on a one-to-one basis has no effect on the TPI_{12} signal.

The second method for determining the rate coef-

ficient k_{12} makes use of the profiles in Fig. 5 measured with the 0.1 M solution of higher concentration in the atomizer. The flat plateau values downstream for all five FR flames demonstrate that ion production is equal to ion loss, i.e. $d[TPI_{90}]/dz = 0$ for the yttrium ions. Thus, the kinetic expression reduces to $k_{12}[OYOH][H] = k_{12}\{[Y_{tot}]K_1[H_2O]/(\gamma + K_1[H_2O]/[H]_{eq})\}\gamma = k_{-12}[TPI_{90}]^2$ with $K_1 = \exp(-49{,}000/RT)$. At this higher concentration of 0.1 M, the $k_2[H]^2[OH]$ production term for H_3O^+ is negligible. By using flame 3 as an example, $k_{12} = 6.2 \times 10^{-17}$ cm^3 molecule^{-1} s^{-1}. The results of these determinations of k_{12} for the five FR flames are presented in Fig. 9 as a plot of ln k_{12} versus $1/T$ (filled circles, solid line). The least-squares fit of a straight line through the data points yields $k_{12} = (2.7 \pm 0.8) \times 10^{-12} \exp(-22452/T)$ cm^3 molecule^{-1} s^{-1}. These results of the second method are more reliable than those of the first, and they are the values that we advocate. In the first method, the experimental results and their interpretation as well as the method of data analysis by curve fitting are more elaborate and, consequently, more prone to errors. The first method was necessary, however, in order to arrive at a satisfactory value of the equilibrium constant K_1 for application to the second method.

4. Summary and conclusions

Premixed H_2–O_2–N_2 flames in the temperature range 1820–2400 K were employed for this work. In hydrogen flames, the radical concentrations in the reaction zone exceed their equilibrium values by a factor γ known as the disequilibrium parameter, which decays downstream towards unity in the burnt gas; e.g. $[H] = \gamma[H]_{eq}$ in FR flames. The group 3 (or 3B) metals Sc, Y, and La ionize in these flames, and Y was chosen to investigate the ionization processes. The dominant neutral yttrium species in the flames are OYOH and YO, linked by the balanced reaction $YO + H_2O = OYOH + H$; because [H] is involved, [OYOH]/[YO] depends on γ and varies along the flame axis. The equilibrium constant of the balanced reaction was determined to be $K_1 = \exp(-49{,}000/RT)$ so that [OYOH] > 80% for the fuel-rich flames studied here; the % increases with decreasing temperature (and is higher in a fuel-lean flame at the same temperature). This is consistent with a bond energy D^0(OY–OH) = 449 ± 20 kJ mol^{-1} (4.65 ± 0.21 eV), 50 kJ mol^{-1} stronger than D^0(OY–O) = 399 ± 40 kJ mol^{-1} (4.14 ± 0.41 eV). Although YO^+ is observed at the limit of detection, $Y(OH)_2^+$ (isomeric with $YO^+ \cdot H_2O$) is believed to be the primary ion; higher hydrate ions observed with the mass spectrometer arise primarily through cooling during passage through the sampling nozzle. The recombination coefficient k_7 or $k_{-12} = (9.7 \pm 1.5)T^{-2.3 \pm 0.6}$ cm^3 molecule^{-1} s^{-1} for electron-ion recombination of $Y(OH)_2^+$ was measured over the temperature range 1820–2400 K corresponding to values of 3.1–1.6 × 10^{-7}, respectively, typical of so many simple molecular ions in flames. The relatively weak $T^{-2.3\pm0.6}$ temperature dependence has rather large error limits such that it is in approximate agreement with the $T^{-1.5}$ dependence expected from simple theory.

Yttrium ion production appears to occur primarily by way of chemi-ionization of OYOH with H. If there is a contribution from collisional (thermal) ionization of YO that has a low ionization energy, it should amount to <1%. Analysis of the ion profiles as a function of γ is a useful method for establishing the ionization mechanism. The rate constant for chemi-ionization $k_{12} = (2.7 \pm 0.8) \times 10^{-12} \exp(-22452/T)$ cm^3 molecule^{-1} s^{-1} gives values in the range (1.2–23.4) × 10^{-17} corresponding to 1820–2400 K, respectively, with the expected positive temperature dependence. These values are small compared with those for the chemi-ionization of strontium (one atomic number lower) by Sr + OH and/or SrO + H, which gives (1.1–14.4) × 10^{-14} cm^3 molecule^{-1} s^{-1} for the same temperature range [26], larger by a factor of 600 or more. Finally, it should be stated that the values of k_{12} are lower limits because an unknown fraction, presumably small, of the total yttrium introduced into the flames might be present as solid particles. In view of this study, further work of a similar nature on scandium and lanthanum is contemplated in order to establish trends in the chemical kinetics of the group 3 (or 3B) metallic ions.

Acknowledgement

Support of this work by the Natural Sciences and Engineering Research Council of Canada is gratefully acknowledged.

References

[1] P.M. Patterson, J.M. Goodings, Int. J. Mass Spectrom. Ion Processes 148 (1995) 55.
[2] P.M. Patterson, J.M. Goodings, Int. J. Mass Spectrom. Ion Processes 152 (1996) 43.
[3] A.F. Ashton, A.N. Hayhurst, Combust. Flame, 21 (1973) 69.
[4] M.W. Chase, Jr., C.A. Davies, J.R. Downey, Jr., D.J. Frurip, R.A. McDonald, A.N. Syverud, JANAF Thermochemical Tables, 3rd ed., J. Phys. Chem. Ref. Data 14 (Suppl.1) (1985).
[5] C.J. Butler, A.N. Hayhurst, J. Chem. Soc., Faraday Trans. 93 (1997) 1497.
[6] A.N. Hayhurst, D.B. Kittelson, Proc. R. Soc. London, Ser. A 338 (1974) 155.
[7] J.M. Goodings, C.S. Hassanali, P.M. Patterson, C. Chow, Int. J. Mass Spectrom. Ion Processes 132 (1994) 83.
[8] J.M. Goodings, S.M. Graham, W.J. Megaw, J. Aerosol Sci. 14 (1983) 679.
[9] D.R. Lide (Ed.),CRC Handbook of Chemistry and Physics, 73rd ed., CRC, Boca Raton, FL, 1992.
[10] R. Kelly, P.J. Py, Trans. Faraday Soc. 65 (1969) 367.
[11] J.M. Goodings, P.M. Patterson, Int. J. Mass Spectrom. Ion Processes 151 (1995) 17.
[12] S.D.T. Axford, A.N. Hayhurst, Int. J. Mass Spectrom. Ion Processes 110 (1991) 31.
[13] A.N. Hayhurst, D.B. Kittelson, N.R. Telford, Combust. Flame 28 (1977) 123.
[14] A.N. Hayhurst, D.B. Kittelson, Combust. Flame 28 (1977) 137.
[15] N.A. Burdett, A.N. Hayhurst, Combust. Flame 34 (1979) 119.
[16] J.B. Pedley, E.M. Marshall, J. Phys. Chem. Ref. Data 12 (1983) 967.
[17] P.N. Crovisier, J.H. Horton, C.S. Hassanali, J.M. Goodings, Can. J. Chem. 70 (1992) 839.
[18] T.M. Sugden, Trans. Faraday Soc. 52 (1956) 1465.
[19] D.E. Clemmer, N.F. Dalleska, P.B. Armentrout, Chem. Phys. Lett. 190 (1992) 259.
[20] S.D.T. Axford, A.N. Hayhurst, J. Chem. Soc., Faraday Trans. 91 (1995) 827.
[21] S.G. Lias, J.E. Bartmess, J.F. Liebman, J.L. Holmes, R.D. Levin, W.G. Mallard, J. Phys. Chem. Ref. Data 17 (Suppl. 1) (1988).
[22] A.N. Hayhurst, N.R. Telford, Trans. Faraday Soc. 66 (1970) 2784.
[23] C.J. Butler, A.N. Hayhurst, J. Chem. Soc., Faraday Trans. 92 (1996) 707.
[24] M.C. R. Cockett, J.M. Dyke, A.M. Ellis, M. Fehér, T.G. Wright, J. Electron Spectrosc. Relat. Phenom. 51 (1990) 529.
[25] J.M. Goodings, A.N. Hayhurst, J. Chem. Soc., Faraday Trans. 2, 84 (1988) 745.
[26] A.N. Hayhurst, D.B. Kittelson, Proc. R. Soc. London, Ser. A 338 (1974) 175.